

Binary and ternary copper(II) complexes of a new Schiff base ligand derived from 4-acetyl-5,6-diphenyl-3(2H)-pyridazinone: Synthesis, spectral, thermal, antimicrobial and antitumor studies

Magdy Shebl*, Omima M.I. Adly, Ebtesam M. Abdelrhman, B.A. El-Shetary

Department of Chemistry, Faculty of Education, Ain Shams University, Roxy, Cairo, Egypt



ARTICLE INFO

Article history:

Received 22 December 2016

Received in revised form

12 May 2017

Accepted 14 May 2017

Available online 18 May 2017

Keywords:

Pyridazinone

Binary and ternary complexes

Schiff base

Thermodynamic parameters

Antimicrobial activity

Antitumor activity

ABSTRACT

A new Schiff base ligand was synthesized by the reaction of 4-acetyl-5,6-diphenyl-3(2H)-pyridazinone with ethylenediamine. A series of binary copper(II) Schiff base complexes have been synthesized by using various copper(II) salts; AcO^- , NO_3^- , ClO_4^- , Cl^- and Br^- . Ternary complexes were synthesized by using auxiliary ligands (L') [N,O-donor; 8-hydroxyquinoline and glycine or N,N-donor; 1,10-phenanthroline, bipyridyl and 2-aminopyridine]. The structures of the Schiff base and its complexes were characterized by elemental and thermal analyses, IR, electronic, mass, ^1H NMR and ESR spectra in addition to conductivity and magnetic susceptibility measurements. The obtained complexes include neutral binuclear complexes as well as neutral and cationic mononuclear complexes according to the anion used and the experimental conditions. The ESR spin Hamiltonian parameters of some complexes were calculated and discussed. The metal complexes exhibited octahedral and square planar geometrical arrangements depending on the nature of the anion. Kinetic parameters (E_a , A , ΔH , ΔS and ΔG) of the thermal decomposition stages were evaluated using Coats–Redfern equations. The antimicrobial activity of the Schiff base and its complexes was screened against Gram-positive bacteria (*Staphylococcus aureus* and *Bacillus subtilis*), Gram-negative bacteria (*Salmonella typhimurium* and *Escherichia coli*), yeast (*Candida albicans*) and fungus (*Aspergillus fumigatus*). The antitumor activity of the Schiff base and some of its Cu(II) complexes was investigated against HepG-2 cell line.

© 2017 Elsevier B.V. All rights reserved.

1. Introduction

Schiff bases are considered to be the most important chelating agents in coordination chemistry. Schiff bases and their metal complexes have attracted an enormous consideration because of their various applications including antimicrobial [1], antioxidant [2], anti-inflammatory [3], anticancer [4], antiviral [5] and anti-HIV [6] activities.

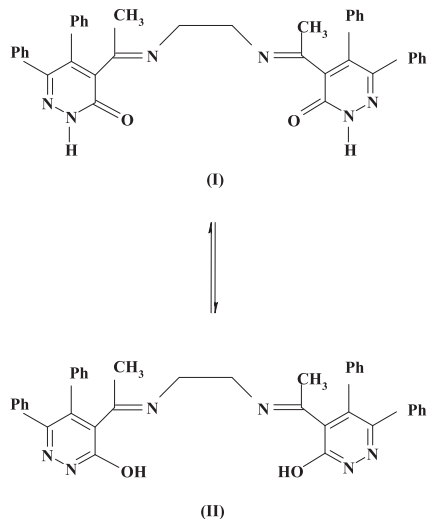
There is a considerable interest in heterocyclic diazines including pyrazine, pyrimidine and pyridazine as excellent bidentate chelating agents [7]. Pyridazines, and particularly 3-pyridazinone derivatives possess antibacterial [8], antifungal [9], anticancer [10], antitubercular [9], anti-inflammatory and analgesic [11], antihypertensive [12] as well as various pharmacological activities [13].

Copper(II) ion plays very important roles in several biological processes. It has a significant role in the action of different enzymes that catalyze a great variety of reactions [14]. Copper(II) complexes have been extensively studied because of their biological and pharmaceutical properties [15]. It has also been reported that the biological activity of copper(II) complexes is enhanced in the presence of a nitrogen donor heterocyclic ligand, such as 1,10-phenanthroline, 2,2'-bipyridine or 2,2'-dipyridylamine [16].

The present study aims to study the chelating behavior of the new Schiff base, *N,N'*-bis[5,6-diphenyl-3-oxo-2H-pyridazin-3-yl-ethylidene]ethane-1,2-diamine (**Scheme 1**) towards copper(II) ion. A series of binary and ternary complexes have been synthesized and characterized by elemental and thermal analyses, IR, electronic, ESR and mass spectra as well as conductivity and magnetic susceptibility measurements. The antimicrobial activity of the ligand and its complexes was screened against selected kinds of bacteria and fungi. The antitumor activity of the ligand and some of its Cu(II) complexes was investigated against HepG2 cell line.

* Corresponding author.

E-mail address: magdy.shebl@hotmail.com (M. Shebl).



Scheme 1. Tautomeric forms of the Schiff base ligand.

2. Experimental

2.1. Measurements

Elemental analyses (C, H and N) were carried out using Vario El-Elementar at the Ministry of Defense, Chemical War Department. Analysis of the metal content followed the decomposition of the complexes with conc. nitric acid then copper(II) ion was estimated by EDTA. Melting points of the complexes were determined using a Stuart SMP3 melting point apparatus. IR spectra were recorded using KBr discs on FT IR Nicolet IS10 spectrometer. Electronic spectra were recorded at room temperature on a Jasco model V-550 UV/Vis spectrophotometer as Nujol mulls and/or solutions in DMF. ¹H NMR spectra were recorded at room temperature on a Bruker WP 200 SY spectrometer. Dimethylsulfoxide, DMSO-*d*₆, was used as a solvent and tetramethylsilane as an internal reference. ESR spectra of the complexes were recorded at Elexsys, E500, Bruker company. The magnetic field was calibrated with 2,2'-diphenyl-1-picrylhydrazyl (DPPH) sample purchased from Aldrich. Mass spectra were recorded at 70 eV on a Gas chromatographic GCMSQp 1000 ex Shimadzu instrument. The magnetic susceptibility measurements were carried out at room temperature using a magnetic susceptibility balance of the type Johnson Matthey, Alfa product, Model No. (MKI). Effective magnetic moments were calculated and corrected using Pascal's constants for the diamagnetism of all atoms in the compounds [17]. Molar conductivities were measured for 10⁻³ M solution of the solid complexes on the Corning conductivity meter NY 14831 model 441. TGA-measurements were carried out from room temperature up to 800 °C at a heating rate of 10 °C/min on a Shimadzu-50 thermal analyzer.

2.2. Materials

4-Acetyl-5,6-diphenyl-3(2H)-pyridazinone was prepared according to literature [18]. Metal salts, 8-hydroxyquinoline, glycine, 1,10-phenanthroline, bipyridyl, 2-aminopyridine and EDTA disodium salt, ammonium hydroxide, mureoxide and nitric acid were either Aldrich, BDH or Merck products. Organic solvents were reagent grade chemicals and were used without further purification. Crystal violet and trypan blue dye were purchased from Sigma (St. Louis, Mo., USA). Fetal Bovine serum, DMEM, RPMI-1640, HEPES buffer solution, L-glutamine, gentamycin and 0.25% Trypsin-EDTA

were obtained from Lonza. HepG-2 cells (human Hepatocellular carcinoma) were obtained from VACSER A Tissue Culture Unit.

Caution! Perchlorate salts are potentially explosive especially in the presence of organic ligands. Only a small amount should be prepared and handled with care.

2.3. Synthesis of the Schiff base ligand

The Schiff base ligand was synthesized by adding ethylenediamine (0.1 g, 1.66 mmol) dissolved in absolute ethanol (10 mL) to 4-acetyl-5,6-diphenyl-3(2H)-pyridazinone (1 g, 3.44 mmol) in absolute ethanol (20 mL). The reaction mixture was heated under reflux for 2 h. The obtained yellow product was filtered off and washed with few amounts of ethanol then diethylether, air-dried and recrystallized from methanol-DMF. The crystalline ligand was kept in a desiccator until used. The yield was 0.8 g (38%).

2.4. Synthesis of the metal complexes

The metal salt and the ligand, both in ethanol, were mixed in the molar ratio 1:2 (L:M) and heated under reflux for 4 h. In order to investigate the experimental conditions, reactions of the ligand with copper(II) chloride or bromide were carried out using stirring conditions in addition to the regular reflux method. The resulting precipitates were filtered, washed with ethanol then ether and finally air-dried. The complexes were kept in a desiccator over anhydrous calcium chloride. As representative examples, the following synthetic methods are provided in details.

2.4.1. Synthesis of [(L)Cu₂(OAc)₄(H₂O)₄]-EtOH (1)

0.264 g (1.32 mmol) of Cu(OAc)₂·H₂O dissolved in 30 mL ethanol was added gradually to 0.4 g (0.66 mmol) of the ligand, suspended in 30 mL ethanol. The reaction mixture was heated under reflux for 4 h which resulted a dark brown precipitate and was filtered off, washed several times with ethanol, diethylether and finally air-dried. The yield was 32%.

2.4.2. Synthesis of [(L)Cu₂(OAc)₂(8-HQ)₂(H₂O)₂] (8)

0.66 g (3.3 mmol) of Cu(OAc)₂·H₂O dissolved in 40 mL ethanol was added gradually to 1 g (1.65 mmol) of the ligand, suspended in 40 mL ethanol. The reaction mixture was heated under reflux for 30 min and then 0.48 g (3.3 mmol) of 8-hydroxyquinoline (8-HQ) dissolved in ethanol was added to the above mixture. The resulting mixture was heated under reflux 7 h which resulted a dark green precipitate and was filtered off, washed several times with ethanol, diethylether and finally air-dried. The yield was 29%.

2.4.3. Unsuccessful trials

Trials to prepare the binary Cu(II) complex of the Schiff base ligand by using Cu(II) sulphate were unsuccessful.

2.5. Biological activity

2.5.1. Antimicrobial activity

The standardized disc agar diffusion method [19] was followed to determine the activity of the Schiff base and its metal complexes against the sensitive organisms *Staphylococcus aureus* (ATCC 25923) and *Bacillus subtilis* (ATCC 6635) as Gram positive bacteria, *Salmonella typhimurium* (ATCC 14028) and *Escherichia coli* (ATCC 25922) as Gram negative bacteria and *Candida albicans* (ATCC 10231) and *Aspergillus fumigatus* as fungus strain. The antibiotic chloramphenicol was employed as reference in the case of Gram-positive bacteria, cephalothin in the case of Gram-negative bacteria and cycloheximide in the case of fungi.

2.5.2. Antitumor activity

Antitumor activity was monitored on HepG-2 cells by determining the effect of the test samples on cell morphology and cell viability according to literature method [20].

3. Results and discussion

3.1. The Schiff base ligand

Table 1 summarizes the analytical and physical data of the Schiff base ligand and its metal complexes. The results of the elemental analyses are in a good agreement with the proposed formula.

The characteristic infrared spectral data of the Schiff base ligand and its metal complexes are scheduled in **Table 2**. The IR spectrum of the ligand showed four bands at 3289, 1665, 1572 and 1537 cm⁻¹ that may be assigned to $\nu(\text{NH})$, $\nu(\text{C}=\text{O})$, $\nu(\text{C}=\text{N})$ and $\nu(\text{C}=\text{C})$, respectively.

The electronic spectral data of the ligand in DMF (**Table 3**) showed two bands at 271 and 328 nm. The higher energy band may be assigned to $\pi-\pi^*$ transitions of the azomethine linkage and the aromatic benzene ring. The lower energy band may be assigned to the $n-\pi^*$ transition which is overlapped with charge transfer transitions within the molecule.

¹H NMR spectral data (δ ppm) of the ligand relative to TMS (0 ppm) in DMSO-*d*₆ are summarized in **Table 4**. The signals observed at 12.58 ppm may be assigned to the NH protons. The signals due to aromatic protons are detected in the range 7.00–7.28 ppm. Finally, signals observed at 2.84 and 1.78 ppm may be assigned to the CH₂ and CH₃ protons, respectively.

The mass spectrum of the Schiff base (**Fig. 1**) showed the molecular ion peak at *m/z* 605, confirming its formula weight (F.W. 604.72). The mass fragmentation pattern, shown in **Scheme S1** (Supplementary material), supported the suggested structure of the ligand.

3.2. Metal complexes

The ligand reacted with several Cu(II) salts of ACO⁻, NO₃⁻, Cl⁻, Br⁻ and ClO₄⁻ in order to determine the effect of the anion on the products. Also, the ligand was allowed to react with copper(II) ion in the presence of secondary ligands (L') [N,O-donor; 8-hydroxyquinoline and glycine or N,N-donor; 1,10-phenanthroline, bipyridyl and 2-aminopyridine]. The prepared complexes are quite stable at room temperature, non-hygroscopic and insoluble in water and common organic solvents. The obtained complexes are characterized by elemental and thermal analyses, IR, electronic, ESR and mass spectra as well as conductivity and magnetic measurements. The analytical data of the complexes are scheduled in **Table 1**.

3.2.1. IR spectra

The IR spectral data of the complexes are scheduled in **Table 2**. The IR spectra of the metal complexes showed a broad band in the range 3378–3455 cm⁻¹ assignable to $\nu(\text{OH})$ of the coordinated or uncoordinated water and/or ethanol molecules associated with the complexes. The band observed in the range 3130–3320 cm⁻¹ may be assigned to $\nu(\text{NH})$. Also, the bands at 1665 and 1572 cm⁻¹ assigned to $\nu(\text{C}=\text{O})$ and $\nu(\text{C}=\text{N})$, respectively in the free ligand were shifted to lower wave number in all complexes, indicating the participation of these groups in chelation [21]. The appearance of $\nu(\text{NH})$ and $\nu(\text{C}=\text{O})$ bands suggests the presence of the ligand in the pyridazinone form (tautomer I, **Scheme 1**) in the solid state. In complexes **1**, **8–12**, the new bands observed in the ranges 1430–1481 and 1201–1227 cm⁻¹ may be due to $\nu_{\text{as}}(\text{COO}^-)$ and $\nu_s(\text{COO}^-)$, respectively of the acetate group [22]. The band difference ($\Delta\nu = (\nu_{\text{as}} - \nu_s) = 215\text{--}254\text{ cm}^{-1}$) suggests a monodentate nature of the acetate anion [23–26]. Complex **2** showed new bands at 1384 and 826 cm⁻¹, indicating the ionic nature of the NO₃⁻ group [27–32]. In complex **3**, the new bands observed at 1092 and

Table 1
Analytical and physical data of the pyridazinone Schiff base and its complexes.

No.	Reaction	Complex M. F. [F. Wt]	Color	Yield (%)	M.P. °C	Elemental analysis, % Found/(Calc.)				
						C	H	N	Cl/Br	M
(1)	L + Cu(OAc) ₂ ·H ₂ O	C ₃₈ H ₃₂ N ₆ O ₂ [604.72] [(L)Cu ₂ (OAc) ₄ (H ₂ O) ₄]·EtOH C ₄₈ H ₅₈ N ₆ O ₁₅ ·Cu ₂ [1086.12]	Yellow Dark brown	38 32	>300 >300	75.3 (75.48) 53.5 (53.08)	5.12 (5.33) 5.0 (5.38)	13.8 (13.90) 7.83 (7.74)	— 11.6 (11.70)	
(2)	L + Cu(NO ₃) ₂ ·3H ₂ O	[(L)Cu](NO ₃) ₂ ·0.5EtOH C ₃₉ H ₅₅ N ₅ O _{8.5} Cu [815.51]	Green	48	235	57.03 (57.45)	5.16 (4.33)	12.58 (13.74)	7.40 (7.79)	
(3)	L + Cu(ClO ₄) ₂ ·6H ₂ O	[(L)Cu(H ₂ O) ₂](ClO ₄) ₂ ·3.5H ₂ O C ₃₈ H ₄₃ N ₆ O _{15.5} Cl ₂ Cu [966.25]	Green	31	a	47.03 (47.24)	4.45 (4.49)	7.79 (8.70)		^a (6.58)
(4)	L + CuCl ₂ ·2H ₂ O	[(L)Cu ₂ Cl ₄ (H ₂ O) ₄] C ₃₈ H ₄₀ N ₆ O ₆ Cl ₄ Cu ₂ [945.68]	Pale green	21	225	48.5 (48.26)	4.5 (4.26)	9.1 (8.89)	(15.0)	13.2 (13.44)
(5)	L + CuCl ₂ ·2H ₂ O (stirring)	[(L)CuCl ₂] C ₃₈ H ₃₂ N ₆ O ₂ Cl ₂ Cu [739.17]	Pale green	64	210	62.0 (61.75)	4.76 (4.36)	11.6 (11.37)	(9.59)	8.4 (8.6)
(6)	L + CuBr ₂	[(L)Cu ₂ Br ₄]·0.5EtOH C ₃₉ H ₃₅ N ₆ O _{2.5} Br ₂ Cu ₂ [1074.46]	Dark green	52	215	43.8 (43.6)	3.0 (3.28)	7.7 (7.82)	(29.75)	11.6 (11.83)
(7)	L + CuBr ₂ (stirring)	[(L)CuBr ₂]·0.5EtOH C ₃₉ H ₃₅ N ₆ O _{2.5} Br ₂ Cu [851.11]	Orange	68	202	54.6 (55.04)	4.0 (4.15)	10 (9.87)	(18.78)	7.2 (7.47)
(8)	L + Cu(OAc) ₂ ·H ₂ O + 8-HQ	[(L)Cu ₂ (OAc) ₂ (8-HQ) ₂ (H ₂ O) ₂] C ₆₀ H ₅₄ N ₈ O ₁₀ Cu ₂ [1174.24]	Dark green	29	>300	62.17 (61.37)	4.05 (4.64)	9.2 (9.54)	10.8 (10.82)	
(9)	L + Cu(OAc) ₂ ·H ₂ O + Gly	[(L)Cu ₂ (OAc) ₂ (Gly) ₂ (H ₂ O) ₂]·5H ₂ O C ₄₆ H ₆₀ N ₈ O ₁₂ Cu ₂ [1124.13]	Grey	16	>300	48.66 (49.15)	4.91 (5.38)	10.52 (9.97)	11.0 (11.31)	
(10)	L + Cu(OAc) ₂ ·H ₂ O + Phen	[(L)Cu ₂ (OAc) ₄ (Phen) ₂]·2EtOH C ₇₄ H ₇₂ N ₁₀ O ₁₂ Cu ₂ [1420.55]	Dark green	13	192	62.9 (62.57)	5.20 (5.11)	9.99 (9.86)	8.7 (8.95)	
(11)	L + Cu(OAc) ₂ ·H ₂ O + 2,2'-Bipyridyl	[(L)Cu ₂ (OAc) ₄ (Bipy) ₂] C ₆₆ H ₆₀ N ₁₀ O ₁₀ Cu ₂ [1280.37]	Dark brown	17	216	62.2 (61.91)	4.8 (4.72)	10.7 (10.94)	9.7 (9.93)	
(12)	L + Cu(OAc) ₂ ·H ₂ O + 2-Aminopy	[(L)Cu ₂ (OAc) ₄ (Aminopy) ₂ (H ₂ O) ₂]·1.5EtOH·0.5H ₂ O C ₅₉ H ₇₀ N ₁₀ O ₁₄ Cu ₂ [1270.37]	Dark green	28	165	56.05 (55.78)	5.17 (5.55)	10.8 (11.03)	9.8 (10.0)	

^a Not determined.

Table 2

Characteristic IR spectral data of the pyridazinone Schiff base and its complexes.

No. Complex	IR Spectra (cm^{-1})							
	$\nu(\text{OH})$	$\nu(\text{NH})$	$\nu(\text{C=O})$	$\nu(\text{C=N})$	$\nu(\text{C=C})$	$\nu(\text{M-O})$	$\nu(\text{M-N})$	Other bands
L	—	3289	1665	1572	1537	—	—	
1 $[(\text{L})\text{Cu}_2(\text{OAc})_4(\text{H}_2\text{O})_4]\cdot\text{EtOH}$	3418	3196	1644	1567	1500	620	470	$1481\nu_{\text{as}}(\text{COO}^-)$, $1227\nu_{\text{s}}(\text{COO}^-)$; (monodentate OAc^-)
2 $[(\text{L})\text{Cu}](\text{NO}_3)_2\cdot 0.5\text{EtOH}$	3455	3185	1642	1543	—	528	470	1384 , 826 ; $\nu(\text{NO}_3^-)$ (ionic)
3 $[(\text{L})\text{Cu}(\text{H}_2\text{O})_2](\text{ClO}_4)_2\cdot 3.5\text{H}_2\text{O}$	3450	3218	1636	1570	1501	534	446	1092 , 625 ; $\nu(\text{ClO}_4^-)$ (ionic)
4 $[(\text{L})\text{Cu}_2\text{Cl}_4(\text{H}_2\text{O})_4]$	3445	3299	1642	1533	1490	529	471	
5 $[(\text{L})\text{CuCl}_2]$	—	3279	1643	1519	1494	527	478	
6 $[(\text{L})\text{Cu}_2\text{Br}_4]\cdot 0.5\text{EtOH}$	3426	3296	1640	1537	1493	527	486	
7 $[(\text{L})\text{CuBr}_2]\cdot 0.5\text{EtOH}$	3446	3277	1643	1517	1494	525	485	
8 $[(\text{L})\text{Cu}_2(\text{OAc})_2(8-\text{HQ})_2(\text{H}_2\text{O})_2]$	3447	3130	1631	1565	1498	521	406	$1464\nu_{\text{as}}(\text{COO}^-)$, $1223\nu_{\text{s}}(\text{COO}^-)$; (monodentate OAc^-)
9 $[(\text{L})\text{Cu}_2(\text{OAc})_2(\text{Gly})_2(\text{H}_2\text{O})_2]\cdot 5\text{H}_2\text{O}$	3426	3315	1637	1545	1491	515	424	$1440\nu_{\text{as}}(\text{COO}^-)$, $1215\nu_{\text{s}}(\text{COO}^-)$; (monodentate OAc^-)
10 $[(\text{L})\text{Cu}_2(\text{OAc})_4(\text{Phen})_2]\cdot 2\text{EtOH}$	3378	3190	1642	1564	1530	522	431	$1454\nu_{\text{as}}(\text{COO}^-)$, $1224\nu_{\text{s}}(\text{COO}^-)$; (monodentate OAc^-)
11 $[(\text{L})\text{Cu}_2(\text{OAc})_4(\text{Bipy})_2]$	—	3242	1649	1537	1524	518	420	$1442\nu_{\text{as}}(\text{COO}^-)$, $1201\nu_{\text{s}}(\text{COO}^-)$; (monodentate OAc^-)
12 $[(\text{L})\text{Cu}_2(\text{OAc})_4(\text{Aminopy})_2(\text{H}_2\text{O})_2]\cdot 1.5\text{EtOH}\cdot 0.5\text{H}_2\text{O}$	3423	3320	1640	1564	1496	524	424	$1430\nu_{\text{as}}(\text{COO}^-)$, $1215\nu_{\text{s}}(\text{COO}^-)$; (monodentate OAc^-)

Table 3

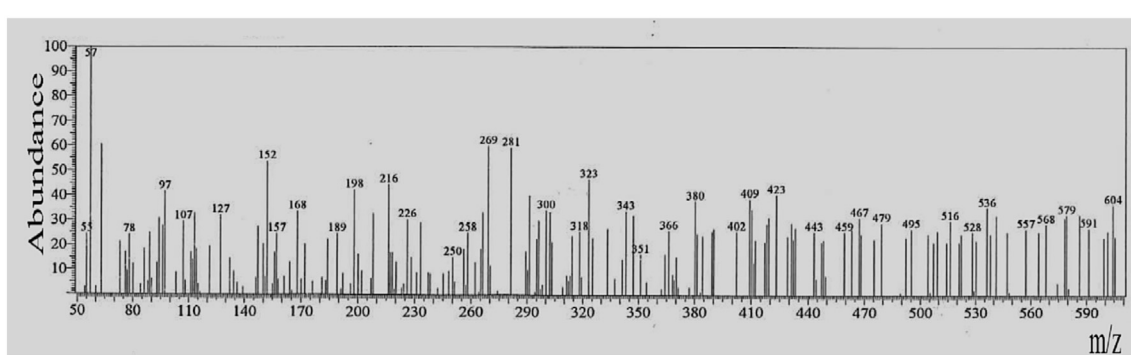
Electronic spectra, magnetic moments and molar conductivity data of the pyridazinone Schiff base and its complexes.

No.	Complex	Electronic spectral bands ^a (nm) $\lambda_{\text{max}}^{\text{a}}$ (nm)/ [$\epsilon_{\text{max}} \text{ L cm}^{-1} \text{ mol}^{-1}$]	$\mu_{\text{eff.}}^{\text{d}}$ B.M.	$\mu_{\text{compl.}}^{\text{e}}$ B.M.	Conductance ^a ($\Omega^{-1} \text{ cm}^2 \text{ mol}^{-1}$)
L		271 [1.04], 328 [0.32]	—	—	—
1 $[(\text{L})\text{Cu}_2(\text{OAc})_4(\text{H}_2\text{O})_4]\cdot\text{EtOH}$	(475,558) ^b (381,588 sh) ^c	1.1	1.5	4.9	
2 $[(\text{L})\text{Cu}](\text{NO}_3)_2\cdot 0.5\text{EtOH}$	(620) ^b	1.69	—	115	
3 $[(\text{L})\text{Cu}(\text{H}_2\text{O})_2](\text{ClO}_4)_2\cdot 3.5\text{H}_2\text{O}$	(615) ^b (362,676 sh) ^c	1.95	—	122	
4 $[(\text{L})\text{Cu}_2\text{Cl}_4(\text{H}_2\text{O})_4]$	(396,446,707) ^c	1.16	1.64	36	
5 $[(\text{L})\text{CuCl}_2]$	(705) ^c	1.9	—	39.9	
6 $[(\text{L})\text{Cu}_2\text{Br}_4]\cdot 0.5\text{EtOH}$	(440,627) ^c	1.83	2.59	50	
7 $[(\text{L})\text{CuBr}_2]\cdot 0.5\text{EtOH}$	(448,553) ^c	2.06	—	46	
8 $[(\text{L})\text{Cu}_2(\text{OAc})_2(8-\text{HQ})_2(\text{H}_2\text{O})_2]$	(428,688) ^b	1.92	2.72	3.8	
9 $[(\text{L})\text{Cu}_2(\text{OAc})_2(\text{Gly})_2(\text{H}_2\text{O})_2]\cdot 5\text{H}_2\text{O}$	(430,622) ^b (410,632sh) ^c	1.62	2.3	3.2	
10 $[(\text{L})\text{Cu}_2(\text{OAc})_4(\text{Phen})_2]\cdot 2\text{EtOH}$	(620) ^b	1	1.45	4	
11 $[(\text{L})\text{Cu}_2(\text{OAc})_4(\text{Bipy})_2]$	(613) ^c	2.35	4.12	9.9	
12 $[(\text{L})\text{Cu}_2(\text{OAc})_4(\text{Aminopy})_2(\text{H}_2\text{O})_2]\cdot 1.5\text{EtOH}\cdot 0.5\text{H}_2\text{O}$	(643) ^b (481,716) ^c	1.55	2.19	6.2	

^a Solutions in DMF (10^{-3} M); values of ϵ_{max} are in square brackets and multiplied by 10^{-4} .^b Nujol mull.^c Concentrated solutions.^d $\mu_{\text{eff.}}$ is the magnetic moment of one cationic species in the complex.^e $\mu_{\text{compl.}}$ is the total magnetic moments of all cations in the complex.**Table 4**¹H NMR spectral data of the ligand.

Chemical shifts in ppm (DMSO)	Assignment
1.78	(s, 6H, 2CH_3)
2.84	(s, 4H, 2CH_2)
7.00–7.28	(m, 20H, Ar-H)
12.58	(bs, 2H, 2NH exchangeable with D_2O)

625 cm^{-1} may be assigned to the ionic ClO_4^- group [33–36]. The mixed-ligand complexes containing 8-hydroxyquinoline (**8**), 1,10-phenanthroline (**10**) and 2,2'-bipyridyl (**11**) showed new bands in the range 1497–1524 cm^{-1} , supporting the coordination of the C=N group of the auxiliary ligands to the metal ion [37–41]. The mixed glycine complex (**9**) showed a new band at 1389 cm^{-1} that may be assigned to $\nu_{\text{s}}(\text{COO}^-)$ of the amino acid [42,43]. However, $\nu_{\text{as}}(\text{COO}^-)$ may be obscured by the high intensity band of C=C stretching

**Fig. 1.** Mass spectrum of the Schiff base ligand.

vibration [42,44]. The mixed 2-aminopyridine complex (**12**) showed a new band at 992 cm^{-1} that may be assigned to pyridine ring breathing mode [45]. The preceding elucidation is further supported by the appearance of new bands at $515\text{--}620$ and $406\text{--}486\text{ cm}^{-1}$ that may be attributed to $\nu(\text{M}-\text{O})$ and $\nu(\text{M}-\text{N})$, respectively [24,25,38,46,47].

3.2.2. Conductivity measurements

The molar conductance values of the complexes (Table 3) showed that all complexes have non electrolytic nature except complexes **2** and **3** which gave molar conductance values = 115 and

$122\text{ }\Omega^{-1}\text{ cm}^2\text{ mol}^{-1}$, respectively, suggesting their 1:2 electrolytic nature [48]. These results are in an agreement with the infrared spectral data that showed the presence of ionic nitrate and perchlorate groups. The comparatively high values of complexes **4**–**7** may be due to the partial dissociation in their DMF solutions [48].

3.2.3. Magnetic measurements and electronic spectra

The magnetic moment values of the complexes (except **1**, **4**, **10** and **11**) are in the range $1.55\text{--}1.92\text{ B.M.}$, which refer to one unpaired electron (d^9) [49,50]. Complexes **1**, **4** and **10** have subnormal

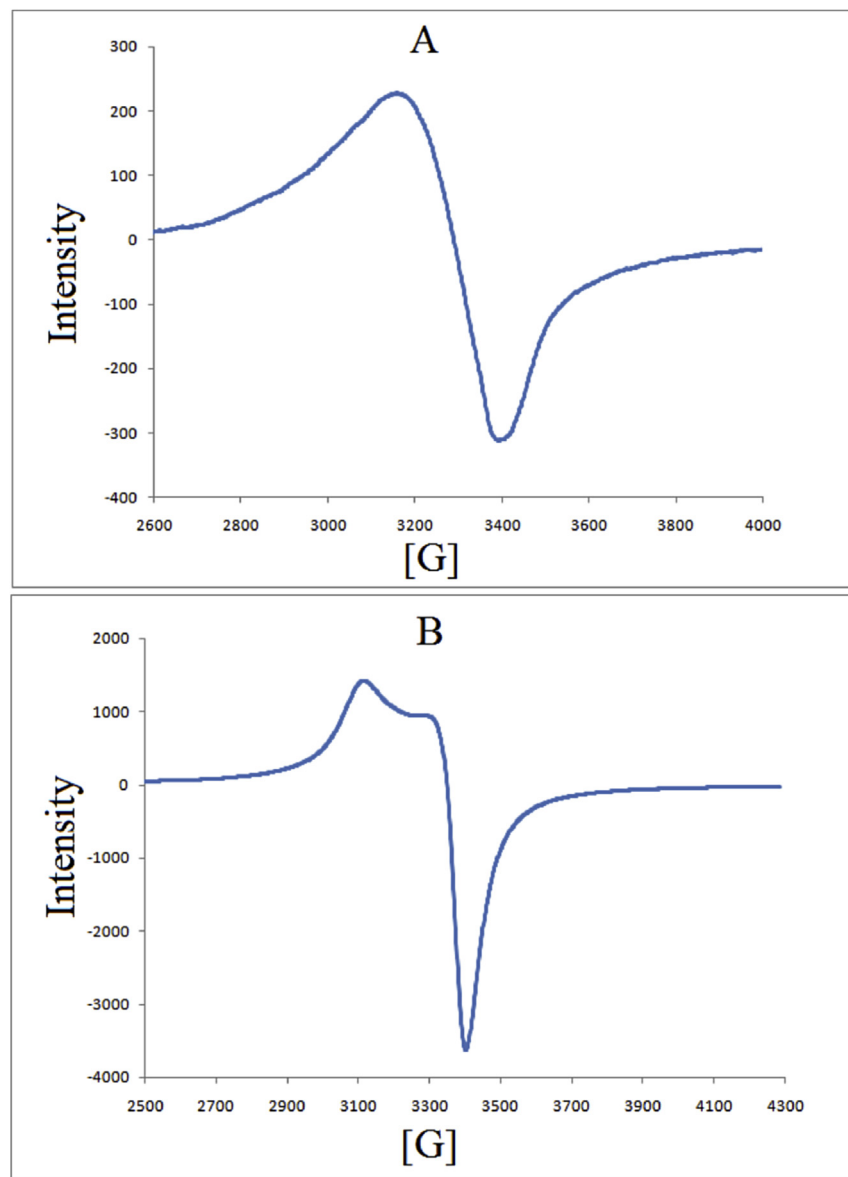


Fig. 2. X-band ESR spectra of the complexes A: $[(\text{L})\text{Cu}](\text{NO}_3)_2\cdot 0.5\text{EtOH}$ (**2**), and B: $[(\text{L})\text{Cu}_2\text{Cl}_4(\text{H}_2\text{O})_4]$ (**4**).

Table 5

ESR data of some copper(II) complexes at room temperature.

Complex	$g\parallel$	g^\perp	$A\parallel \times 10^{-4} (\text{cm}^{-1})$	G	α^2	β^2
$[(\text{L})\text{Cu}_2(\text{OAc})_4(\text{H}_2\text{O})_4]\cdot\text{EtOH}$	2.19	2.08	194	2.4	0.8	0.63
$[(\text{L})\text{Cu}(\text{H}_2\text{O})_2](\text{ClO}_4)_2\cdot 3.5\text{H}_2\text{O}$	2.18	2.08	175	2.3	0.74	0.59
$[(\text{L})\text{Cu}_2\text{Cl}_4(\text{H}_2\text{O})_4]$	2.23	2.06	149	3.8	0.71	0.68

Table 6

Thermal analysis data of some metal complexes.

Complex	DTG peak (°C)	Temperature range (°C)	% Wt. loss Found/(Calc.)	Lost fragment (No. of molecules)
[(L)Cu ₂ (OAc) ₄ (H ₂ O) ₄]·EtOH (1)	71	32–138	4.52/(4.24)	1 EtOH (solv.)
	188	138–208	7.05/(6.73)	4 H ₂ O (coord.)
[(L)Cu](NO ₃) ₂ ·0.5EtOH (2)	55	26–85	2.45/(2.82)	0.5 EtOH (solv.)
	203	100–239	5.61/(5.71)	3 H ₂ O (coord.)
[(L)Cu ₂ Cl ₄ (H ₂ O) ₄] (4)	275	239–403	17.02/(17.34)	1 H ₂ O (coord.) + 4 HCl
	92	45–136	2.33/(2.14)	0.5 EtOH (solv.)
[(L)Cu ₂ Br ₄]·0.5EtOH (6)	213	136–372	7.67/(7.54)	1 HBr
	239	116–257	2.7/(3.07)	2 H ₂ O (coord.)
[(L)Cu ₂ (OAc) ₂ (8-HQ) ₂ (H ₂ O) ₂] (8)	281	257–310	4.88/(5.11)	1 AcOH
	90	44–134	6.67/(6.48)	2 EtOH (solv.)
[(L)Cu ₂ (OAc) ₄ (Phen) ₂]·2EtOH (10)	241	134–296	16.85/(16.89)	4 AcOH
	82	22–128	6.20/(6.14)	1.5 EtOH (solv.) + 0.5H ₂ O (hyd.)

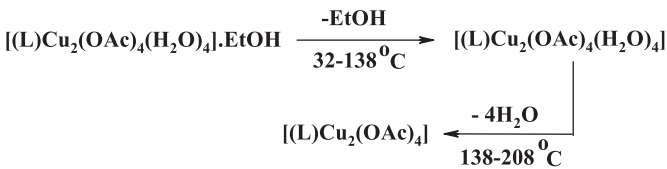
magnetic moment values, which may be due to anti-ferromagnetic interaction [51]. On the other hand, complex **11** has a magnetic moment (2.35 B.M.) higher than the calculated value for one unpaired electron and may be attributed to spin-orbit coupling [51].

The electronic spectra of the complexes (**1**, **3**, **5**, **7–12**) showed an absorption band in the range 553–716 nm, which may be assigned to the $^2E_g \rightarrow ^2T_{2g}$ transition corresponding to a distorted octahedral geometry [52,53]. On the other hand, complexes **2** and **6** showed absorption bands at 620 and 627 nm, respectively, which may be attributed to the $^2B_{1g} \rightarrow ^2A_{1g}$ transition in a square planar geometry [51,53]. In case of some complexes (Table 3), a second band was observed in the range 428–481 nm, which may be due to charge transfer [49].

3.2.4. ESR spectra

ESR spectra of the complexes (**1–4**) were recorded in the solid state. Fig. 2 represents the ESR spectra of complexes **2** and **4**. The spectrum of complex **2** exhibits one broad band with $g = 2.1$ while the spectra of complexes **1**, **3** and **4** exhibit two signals with two g values (Table 5). Based on the profiles of the spectra, octahedral geometry was suggested for complexes **1**, **3** and **4** while square planar for complex **2** [39,54].

The spin Hamiltonian parameters of the complexes were



Scheme 2. Thermal degradation pattern of complex (**1**), $[(\text{L})\text{Cu}_2(\text{OAc})_4(\text{H}_2\text{O})_4]\cdot\text{EtOH}$, in the range of 32–208 °C.

calculated and summarized in Table 5. The room temperature solid state ESR spectra of the complexes are fairly similar and display an axially g-tensor parameters with $g_{||} > g_{\perp} > 2.0023$. The $g_{||}$ value is a significant function for indicating covalent character of M–L bonds [55]; for ionic character, $g_{||} > 2.3$ and for covalent character $g_{||} < 2.3$. For the current complexes, the $g_{||}$ values (Table 5) are less than 2.3 indicating appreciable covalent character for the Cu–L bond. The values of the exchange interaction parameter term G , estimated from the expression $G = (g_{||} - 2)/(g_{\perp} - 2)$ [56], are lower than 4, suggesting copper–copper exchange interactions.

Molecular orbital coefficients, α^2 (a measure of the covalency of the in-plane σ -bonding between copper 3d orbital and the ligand orbitals) and β^2 (covalent in-plane π -bonding), were calculated [57]. The lower values of β^2 compared to α^2 indicate that the in-plane π -bonding is more covalent than the in-plane σ -bonding. These results are in consistent with the data obtained previously [36,53,58].

3.2.5. Thermal analysis

Thermal gravimetric analysis (TGA) is a valuable technique to investigate the nature of associated water or solvent molecules to be either in the inner or outer coordination sphere of the metal ion [59,60]. Moreover, the kinetic and thermodynamic parameters using Coats–Redfern equations have also been calculated. Complexes **1**, **2**, **4**, **6**, **8**, **10** and **12** were taken as ambassador examples for thermal analysis. The results of thermal analysis (Table 6) supported data obtained from elemental analyses.

In case of complex **1**, two decomposition stages were observed in the temperature range 32–208 (Scheme 2), which correspond to the loss of one solvated ethanol and four coordinated water molecules, respectively (weight loss; Calc./Found%; 4.24/4.52 and 6.73/7.05%, respectively).

The thermogram of complex **4** showed two weight losses in the ranges 100–239 and 239–403 °C, which correspond to three

Table 7

Temperatures of decomposition and the kinetic parameters of complexes.

Compound	Step	n order	T (K)	A (S ⁻¹)	ΔE (kJ mol ⁻¹)	ΔH (kJ mol ⁻¹)	ΔS (kJ mol ⁻¹ K ⁻¹)	ΔG (kJ mol ⁻¹)
[(L)Cu ₂ (OAc) ₄ (H ₂ O) ₄]·EtOH	First	1	344	4.4×10^5	27.66	24.799	-0.146	78.018
	Second	0.33	461	16.90	20.037	16.204	-0.233	123.80
[(L)Cu](NO ₃) ₂ ·0.5EtOH	First	1	324	7.33×10^{10}	70.72	68.03	-0.0460	82.95
	Second	0	476	0.494	11.03	7.07	-0.263	132.28
[(L)Cu ₂ Cl ₄ (H ₂ O) ₄]	First	1	548	7.858	17.89	13.33	-0.241	145.50
	Second	1	364.5	1.8×10^5	41.165	38.134	-0.154	94.35
[(L)Cu ₂ Br ₄]·0.5EtOH	First	0.66	486	0.1456	7.379	3.340	-0.270	134.56
	Second	0.5	554	7.089×10^4	59.23	54.62	-0.165	146.36
[(L)Cu ₂ (OAc) ₂ (8-HQ) ₂ (H ₂ O) ₂]	First	0.33	512	22.027	23.87	19.62	-0.232	138.403
	Second	0.5	554	8.014×10^5	10.39	6.11	-0.258	139.033
[(L)Cu ₂ (OAc) ₄ (Phen) ₂]·2EtOH	First	0.5	363	0.236	4.612	1.59	-0.266	98.47
	Second	1	514	0.911	44.22	41.27	-0.142	91.578
[(L)Cu ₂ (OAc) ₄ (Aminopy) ₂ (H ₂ O) ₂]·1.5EtOH·0.5H ₂ O	First	1, 0.33	355	8.014×10^5	44.22	41.27	-0.142	91.578

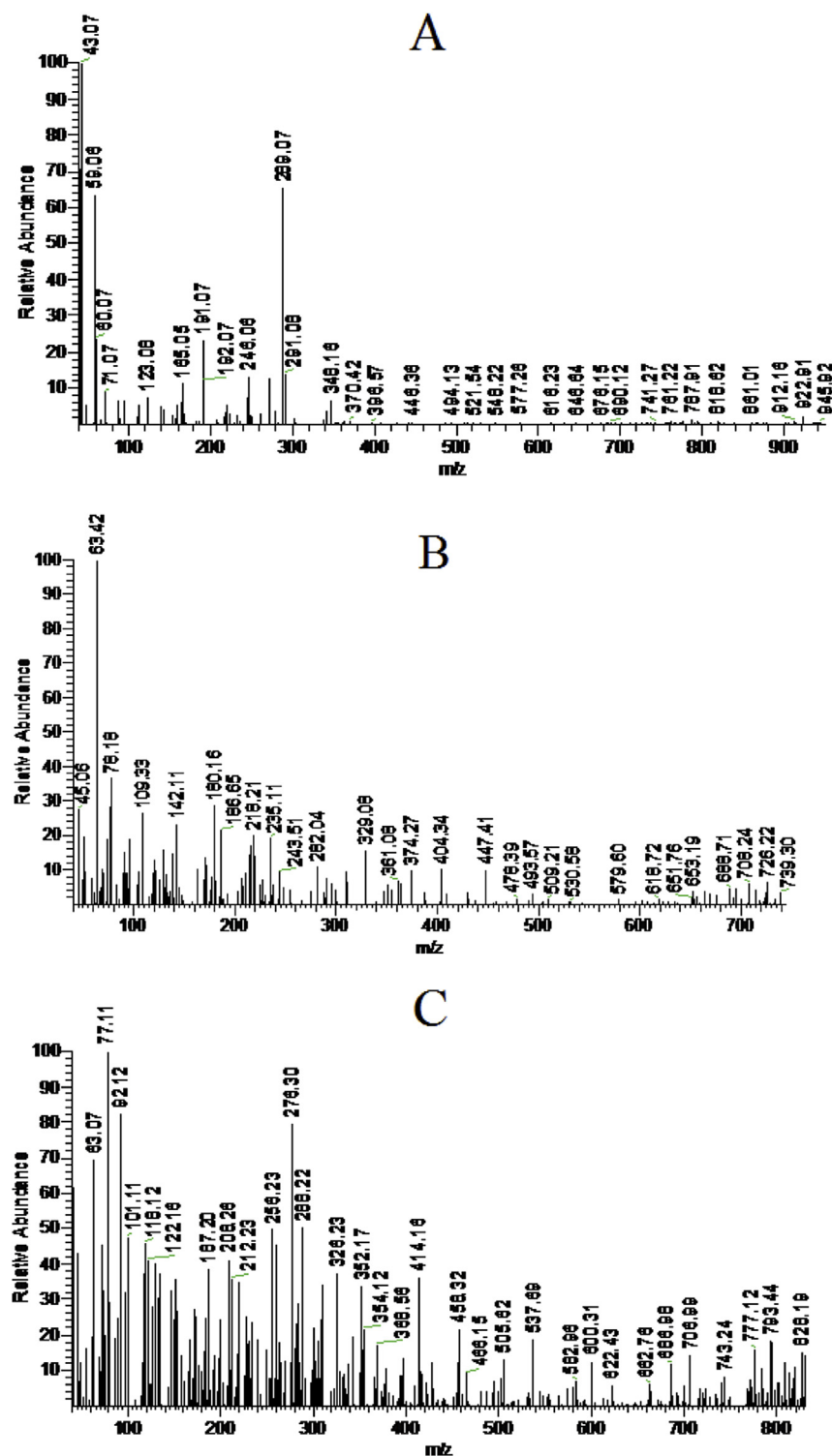


Fig. 3. Mass spectra of the complexes A: $[(L)Cu_2Cl_4(H_2O)_4]$ (4), B: $[(L)CuCl_2]$ (5) and C: $[(L)CuBr_2] \cdot 0.5EtOH$ (7).

coordinated water molecules and one coordinated water in addition to 4HCl molecules (weight loss; Calc./Found%; 5.71/5.61 and 17.34/17.02%, respectively).

The thermogram of complex **6** showed two weight losses in the ranges 45–136 and 136–372 °C, which correspond to half solvated ethanol and one HBr molecules (weight loss; Calc./Found%; 2.14/2.33 and 7.54/7.67%, respectively).

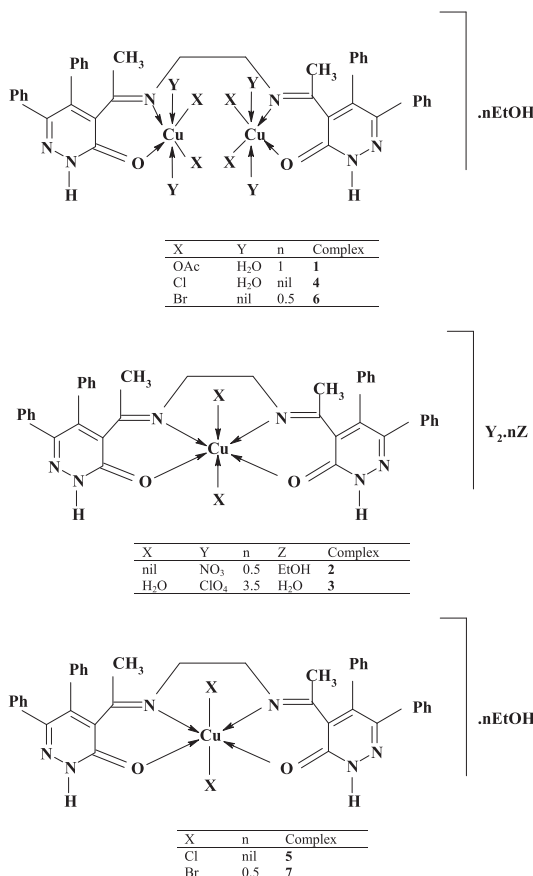
The thermogram of complex **8** showed two weight losses in the ranges 116–257 and 257–310 °C, which correspond to two coordinated water and one AcOH molecules (weight loss; Calc./Found%; 3.07/2.7 and 5.11/4.88%, respectively).

The thermogram of complex **10** showed two weight losses in the ranges 44–134 and 134–296 °C, which correspond to two solvated ethanol and four AcOH molecules (weight loss; Calc./Found%; 6.48/6.67 and 16.89/16.85%, respectively).

Lastly, complexes **2** and **12** showed one decomposition stage in the ranges 26–85 and 22–128 °C, respectively which corresponds to the loss of half solvated ethanol and one and half solvated ethanol in addition to half non-coordinated water molecules, respectively (weight loss; Calc./Found%; 2.82/2.45 and 6.14/6.20%, respectively). However, the coordinated water molecules in complex **12** were lost during the subsequent decomposition stages of the complex.

In order to access the influence of the type of the metal on the thermal behavior of the complexes, the order *n*, and the activation parameters of the various decomposition stages were determined from the TG thermograms using the Coats-Redfern equations [61] in the following forms:

$$\ln[1 - (1-\alpha)^{1-n} / (1-n)T^2] = M/T + B \text{ for } n \neq 1 \quad (1)$$

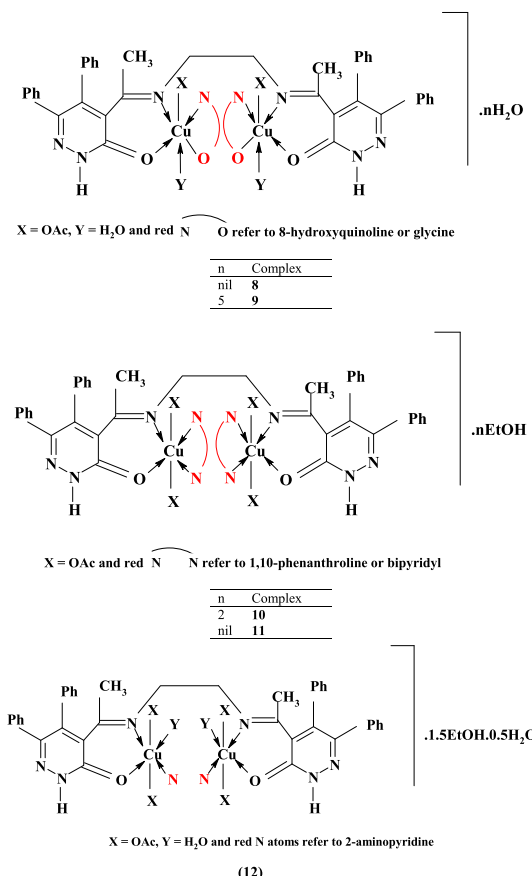


Scheme 3. Representative structures of the binary complexes.

$$\ln[-\ln(1-\alpha)/T^2] = M/T + B \text{ for } n = 1 \quad (2)$$

where *M* = $-E/R$ and *B* = $\ln AR/\Phi E$; *E*, *R*, *A* and Φ are the heat of activation, the universal gas constant, pre-exponential factor and heating rate, respectively.

The correlation coefficient, *r*, was computed using the least square method for different values of *n* = 0, 0.33, 0.5, 0.66, 1 by plotting the left –hand side of Eq. (1) or (2) versus $1000/T$. The *n* values which gave the best fit ($r \approx 1$) was chosen as the order parameter. From the intercept and linear slope of such stage, the *A* and *E* values were determined. The other kinetic parameters ΔH , ΔS and ΔG were computed using the relationships; $\Delta H = E - RT$, $\Delta S = R[\ln(Ah/kT)-1]$ and $\Delta G = \Delta H - T\Delta S$, where *k* is the Boltzmann's constant and *h* is the Plank's constant. The kinetic parameters are listed in Table 7. The following remarks can be pointed out: (1) the positive values of ΔH^* mean that the decomposition processes are endothermic. (2) The energy of activation values *E* for the second step of decomposition of complexes **1** and **6** are lower than the first stage indicating that the rate of decomposition for this stage is higher than the first stage. In case of complexes **4**, **8** and **10**, the second step of decomposition is higher than the first step. This confirms that the rate of decomposition for this stage is lower in the second step [62]. (3) The ΔS^* values for complexes were found to be negative. This indicates that the activated complex is more ordered than the reactants and/or the reactions are slow [63]. (4) The values of ΔG^* are relatively low and of positive sign indicating the autocatalytic effect of metal ions on thermal decomposition of the complexes and non-spontaneous processes [35].



Scheme 4. Representative structures of the ternary complexes.

3.2.6. Mass spectra

The mass spectra of the complexes **4**, **5** and **7** (Fig. 3), as ambassador complexes, support the suggested structures of these complexes. The mass spectra of the complexes **4**, **5** and **7** showed the highest mass peak with *m/z* 946, 739 and 828, respectively which agree very well with the formula weights of complexes **4** [(L) $\text{Cu}_2\text{Cl}_2(\text{H}_2\text{O})_4$] (F. Wt = 945.68) and **5** [(L) CuCl_2] (F. Wt = 739.17) and the anhydrous formula weight of complex **7** [(L) CuBr_2] (F. Wt = 828.11), respectively. The fragmentation patterns of the complexes showed a fragment with *m/z* 604 due to the Schiff base ligand.

Finally, based on the above interpretation of analytical and spectral techniques, tentative structures of the metal complexes can be summarized in Schemes 3 and 4.

3.3. Biological studies

3.3.1. Antimicrobial studies

The antimicrobial activity of the ligand and its metal complexes was investigated against *Staphylococcus aureus* (ATCC 25923) and *Bacillus subtilis* (ATCC 6635) as Gram-positive bacteria, *Escherichia coli* (ATCC 25922) and *Salmonella typhimurium* (ATCC 14028) as Gram-negative bacteria, yeast: *Candida albicans* (ATCC 10231) and fungus: *Aspergillus fumigatus*. The results are listed in Table 8. Inspection of the data given in Table 8 reveals that the ligand is only active towards *Bacillus subtilis* and the complexation process enhanced this activity except for complex **9**. Against *Staphylococcus aureus*, some complexes showed a lower antimicrobial activity. Against *Salmonella typhimurium*, few complexes showed intermediate to higher activity. Against *Escherichia coli*, some complexes showed lower to intermediate activity. Towards *Candida albicans*, all complexes are biologically active with higher activity for most of them. Towards *Aspergillus fumigatus*, some complexes showed lower to intermediate activity.

It was reported that the antibacterial activity of the compound is affected by different factors such as nature of the chelating agent and its chelating sites, nature of the metal ion, geometrical

Table 9

Antitumor activity of the Schiff base ligand and its complexes **1** and **8** against Hep-G2 cell line.

Compound	IC ₅₀ ($\mu\text{g}/\text{ml}$)
L	15.3
[(L) $\text{Cu}_2(\text{OAc})_4(\text{H}_2\text{O})_4 \cdot \text{EtOH}$ (1)	6.53
[(L) $\text{Cu}_2(\text{OAc})_2(8-\text{HQ})_2(\text{H}_2\text{O})_2$] (8)	3.65
Doxorubicin	0.47

IC₅₀ = inhibition concentration 50%.

structure of the complex, solubility and other factors [64].

3.3.2. Antitumor studies

The antitumor activity of the Schiff base ligand and its complexes **1** and **8** was determined *in vitro* against human cancer cell line liver Carcinoma (HEP-G2) and the results are summarized in Table 9. The ligand showed activity towards HEP-G2 and complexes are more active than the free ligand. The higher activity of the complexes than the ligand may be due to the increased conjugation in the ligand skeleton as a result of complex-formation [65].

4. Conclusion

The condensation reaction of 4-acetyl-5,6-diphenyl-3(2H)-pyridazinone with ethylenediamine in molar ratio 2:1 (pyridazinone: ethylenediamine) gave a new pyridazinone Schiff base ligand. A series of binary and ternary copper(II) Schiff base complexes have been synthesized. Schiff base and its complexes were characterized by various analytical and spectroscopic techniques. The obtained complexes are binuclear complexes except for complexes prepared by using NO_3^- or ClO_4^- anions in addition to complexes prepared by stirring (Cl^- and Br^- anions) which are mononuclear complexes. The metal complexes exhibited octahedral and square planar geometrical arrangements. The kinetic and thermodynamic parameters were calculated using Coats-Redfern equations. The antimicrobial activity of the Schiff base and its complexes was

Table 8
Antimicrobial activity of the ligand and its Cu(II) complexes.

Organism	Mean ^a of zone diameter, nearest whole mm.											
	Gram - positive bacteria				Gram - negative bacteria				Yeasts and Fungi ^b			
	<i>S. aureus</i> (ATCC 25923)	<i>B. subtilis</i> (ATCC 6635)	<i>S. typhimurium</i> (ATCC 14028)	<i>E. coli</i> (ATCC 25922)	<i>C. albicans</i> (ATCC 10231)	<i>A. fumigatus</i>						
Concentration	1 mg/ml	0.5 mg/ml	1 mg/ml	0.5 mg/ml	1 mg/ml	0.5 mg/ml	1 mg/ml	0.5 mg/ml	1 mg/ml	0.5 mg/ml	1 mg/ml	0.5 mg/ml
Sample	—	—	9L	7L	—	—	—	—	—	—	—	—
L	—	—	24H	20H	—	—	—	—	30H	24H	9 L	7 L
[(L) $\text{Cu}_2(\text{OAc})_4(\text{H}_2\text{O})_4 \cdot \text{EtOH}$	—	—	22I	16I	—	—	—	—	24H	18I	—	—
[(L) $\text{Cu}(\text{NO}_3)_2 \cdot 0.5\text{EtOH}$	—	—	24H	20H	—	—	—	—	30H	25H	14I	12I
[(L) $\text{Cu}(\text{H}_2\text{O})_2(\text{ClO}_4)_2 \cdot 3.5\text{H}_2\text{O}$	—	—	31 H	27 H	—	—	9L	7L	33H	27H	15I	13I
[(L) $\text{Cu}_2\text{Cl}_2(\text{H}_2\text{O})_4$	9 L	7 L	26H	21H	—	—	16I	13I	31H	27H	—	—
[(L) CuCl_2	—	—	21H	—	—	—	—	—	36H	32H	—	—
[(L) $\text{Cu}_2\text{Br}_2 \cdot 0.5\text{EtOH}$	9L	8L	21I	18H	25H	22H	—	—	28H	25H	—	—
[(L) $\text{CuBr}_2 \cdot 0.5\text{EtOH}$	—	—	22I	18H	—	—	—	—	—	—	—	—
[(L) $\text{Cu}_2(\text{OAc})_2(8-\text{HQ})_2(\text{H}_2\text{O})_2$	12 L	7 L	21 I	15 I	17 I	15 I	9 L	5 L	20 I	14 I	7 L	3 L
[(L) $\text{Cu}_2(\text{OAc})_2(\text{Gly})_2(\text{H}_2\text{O})_2 \cdot 5\text{H}_2\text{O}$	—	—	7 L	3 L	—	—	—	—	8 L	4 L	—	—
[(L) $\text{Cu}_2(\text{OAc})_4(\text{Phen})_2 \cdot 2\text{EtOH}$	8 L	6 L	16 I	11 I	20 I	12 I	10 L	6 L	8 L	5 L	6 L	4 L
[(L) $\text{Cu}_2(\text{OAc})_4(\text{Bipy})_2$	11L	8L	29H	25H	—	—	11L	9L	35H	31H	—	—
[(L) $\text{Cu}_2(\text{OAc})_4(\text{Aminopy})_2 \cdot (\text{H}_2\text{O})_2 \cdot 1.5\text{EtOH} \cdot 0.5\text{H}_2\text{O}$	6 L	5 L	14 I	11 I	19 I	15 I	8 L	5 L	11 L	8 L	—	—
Control ^c	35	26	35	25	36	28	38	27	35	28	37	26

^a Calculated from 3 values.

^b Identified on the basis of routine cultural, morphological and microscopical characteristics. — = No effect. L: Low activity = Mean of zone diameter $\leq 1/3$ of mean zone diameter of control. I: Intermediate activity = Mean of zone diameter $\leq 2/3$ of mean zone diameter of control. H: High activity = Mean of zone diameter $> 2/3$ of mean zone diameter of control.

^c Chloramphenicol in the case of Gram-positive bacteria, cephalothin in the case of Gram-negative bacteria and cycloheximide in the case of fungi.

screened against selected kinds of bacteria and fungi. The Schiff base and most of its complexes showed a promising activity towards *Candida albicans*. The antitumor activity of the ligand and Cu(II) complexes was investigated against HepG2 cell line.

Appendix A. Supplementary data

Supplementary data related to this article can be found at <http://dx.doi.org/10.1016/j.molstruc.2017.05.064>.

References

- [1] (a) A.A. Faheim, S.N. Abdou, Z.H. Abd El-Wahab, Spectrochim. Acta A 105 (2013) 109–124;
(b) N. Raman, S. Sobha, L. Mitu, Monatsh Chem. 143 (2012) 1019–1030.
- [2] (a) H. Wu, G. Pan, Y. Bai, H. Wang, J. Kong, F. Shi, Y. Zhang, X. Wang, J. Coord. Chem. 66 (2013) 2634–2646;
(b) P. Rathi, D.P. Singh, J. Mol. Struct. 1100 (2015) 208–214.
- [3] M.S. Alam, J.H. Choi, D.U. Lee, Bioorg. Med. Chem. 20 (2012) 4103–4108.
- [4] (a) P. Tyagi, S. Chandra, B.S. Saraswat, D. Yadav, Spectrochim. Acta A 145 (2015) 155–164;
(b) X. Li, C. Fang, Z. Zong, L. Cui, C. Bi, Y. Fan, Inorg. Chim. Acta 432 (2015) 198–207.
- [5] (a) K.S. Kumar, S. Ganguly, R. Veerasamy, E. De Clercq, Eur. J. Med. Chem. 45 (2010) 5474–5479;
(b) R. Pignatello, A. Panico, P. Mazzone, M.R. Pinizzotto, A. Garozzo, P.M. Fumeri, Eur. J. Med. Chem. 29 (1994) 781–785.
- [6] S.N. Pandeya, D. Sriram, G. Nath, E. DeClercq, Eur. J. Pharm. Sci. 9 (1999) 25–31.
- [7] (a) S.M.E. Khalil, H.S. Seleem, B.A. El-Shetary, M. Shebl, J. Coord. Chem. 55 (2002) 883–899;
(b) L. Carlusso, G.F. Giani, M. Moret, A. Sironi, J. Chem. Soc. Dalton Trans. (1994) 2397–2404;
(c) F.Z. Mahmoud, A.A.T. Ramadan, D.A. Ali, J. Coord. Chem. 61 (2008) 2639–2654.
- [8] R.R. Kassab, Egypt J. Chem. 45 (2002) 1055–1073.
- [9] I. Mojahidul, A.S. Anees, R. Ramadoss, Acta Pol. Pharm. 65 (2008) 353–362.
- [10] W. Malinka, A. Redzicka, O. Lozach, Farmaco 59 (2004) 457–462.
- [11] D.S. Dogruer, M.F. Sahin, E. Kupeli, E. Yesilada, Turk. J. Chem. 27 (2003) 727–738.
- [12] R. Barbaro, L. Betti, M. Botta, F. Corelli, G. Giannaccini, L. Maccari, F. Manetti, G. Strappaghetti, S. Corsano, J. Med. Chem. 44 (2001) 2118–2132.
- [13] S. Khaidem, S. Sarveswari, R. Gupta, V. Vijayakumar, Int. J. Res. Pharm. Chem. 2 (2012) 258–266.
- [14] (a) Y. Zhang, L. Zhang, L. Liu, J. Guo, D. Wu, G. Xu, X. Wang, D. Jia, Inorg. Chim. Acta 363 (2010) 289–293;
(b) G. Tamasi, L. Chiasserini, L. Savini, A. Segà, R. Cini, J. Inorg. Biochem. 99 (2005) 1347–1359.
- [15] (a) S. Tabassum, A. Asim, F. Arjmand, M. Afzal, V. Bagchi, Eur. J. Med. Chem. 58 (2012) 308–316;
(b) J. Ravichandran, P. Gurumoorthy, M.A.I. Musthafa, A.K. Rahiman, Spectrochim. Acta A 133 (2014) 785–793;
(c) G.-Y. Li, K.-J. Du, J.-Q. Wang, J.-W. Liang, J.-F. Kou, X.-J. Hou, L.-N. Ji, H. Chao, J. Inorg. Biochem. 119 (2013) 43–53.
- [16] (a) C. Dendrinou-Samara, G. Psomas, C.P. Raptopoulou, D.P. Kassis-Soglou, J. Inorg. Biochem. 83 (2001) 7–16;
(b) G. Psomas, C.P. Raptopoulou, L. Iordanidis, C. Dendrinou-Samara, V. Tangoulis, D.P. Kessissoglou, Inorg. Chem. 39 (2000) 3042–3048.
- [17] F.E. Mabbs, D.I. Machin, Magnetism and Transition Metal Complexes, Chapman and Hall, London, 1973.
- [18] V.P. Schmidt, J. Druey, Helv. Chim. Acta 37 (1954) 134–140.
- [19] (a) A.U. Rahman, M.I. Choudhary, W.J. Thomsen, Bioassay Techniques for Drug Development, Harwood Academic Publishers, The Netherlands, 2001;
(b) K.M. Khan, Z.S. Saify, A.K. Zeeshan, M. Ahmed, M. Saeed, M. Schick, H.J. Kohlbau, W. Voelter, Arzneim. Forsch 50 (2000) 915–922.
- [20] (a) T. Mosmann, J. Immunol. Methods 65 (1983) 55–63;
(b) S.M. Gomha, S.M. Riyadh, E.A. Mahmoud, M.M. Elsaeer, Heterocycles 91 (2015) 1227–1243.
- [21] M. Sönmez, İ. Berber, E. Akbaş, Eur. J. Med. Chem. 41 (2006) 101–105.
- [22] K. Nakamoto, Infrared and Raman Spectra of Inorganic and Coordination Compounds, fifth ed., John Wiley and Sons, New York, 1997.
- [23] M. Shebl, Spectrochim. Acta A 117 (2014) 127–137.
- [24] M. Shebl, M. Saif, A.I. Nabeel, R. Shokry, J. Mol. Struct. 1118 (2016) 335–343.
- [25] M. Shebl, J. Coord. Chem. 69 (2016) 199–214.
- [26] H.S. Seleem, B.A. El-Shetary, M. Shebl, Heteroat. Chem. 18 (2007) 100–107.
- [27] N.T. Madhu, P.K. Radhakrishnan, Synth. React. Inorg. Met.-Org. Chem. 31 (2001) 315–330.
- [28] O.M.I. Adly, Spectrochim. Acta A 79 (2011) 1295–1303.
- [29] A.A.A. Emara, O.M.I. Adly, Trans. Met. Chem. 32 (2007) 889–901.
- [30] O.M.I. Adly, A. Taha, J. Mol. Struct. 1038 (2013) 250–259.
- [31] O.M.I. Adly, A. Taha, S.A. Fahmy, J. Mol. Struct. 1054–1055 (2013) 239–250.
- [32] O.M.I. Adly, A.A.A. Emara, Spectrochim. Acta A 132 (2014) 91–101.
- [33] M. Shebl, M.A. Ibrahim, S.M.E. Khalil, S.L. Stefan, H. Habib, Spectrochim. Acta A 115 (2013) 399–408.
- [34] H.S. Seleem, B.A. El-Shetary, S.M.E. Khalil, M. Mostafa, M. Shebl, J. Coord. Chem. 58 (2005) 479–493.
- [35] U. El-Ayaan, I.M. Gabr, Spectrochim. Acta A 67 (2007) 263–272.
- [36] O.M.I. Adly, Spectrochim. Acta A 95 (2012) 483–490.
- [37] M. Shebl, M.A. El-ghamry, S.M.E. Khalil, M.A.A. Kishk, Spectrochim. Acta A 126 (2014) 232–241.
- [38] M. Shebl, S.M.E. Khalil, Monatsh Chem. 146 (2015) 15–33.
- [39] M. Shebl, J. Coord. Chem. 62 (2009) 3217–3231.
- [40] M. Shebl, S.M.E. Khalil, A. Taha, M.A.N. Mahdi, Spectrochim. Acta A 113 (2013) 356–366.
- [41] H.S. Seleem, A.A. Emara, M. Shebl, J. Coord. Chem. 58 (2005) 1003–1019.
- [42] A.M. Shaker, A.M. Awad, L.A.E. Nassr, Synth. React. Inorg. Met.-Org. Chem. 33 (2003) 103–117.
- [43] S. Shobana, J. Dharmaraja, S. Selvaraj, Spectrochim. Acta A 107 (2013) 117–132.
- [44] P. Teyssie, J.J. Charette, Spectrochim. Acta 19 (1963) 1407–1423.
- [45] Z.H. Abd El-Wahab, M.M. Mashaly, A.A. Salman, B.A. El-Shetary, A.A. Faheim, Spectrochim. Acta A 60 (2004) 2861–2873.
- [46] M. Shebl, Spectrochim. Acta A 70 (2008) 850–859.
- [47] M. Shebl, H.S. Seleem, B.A. El-Shetary, Spectrochim. Acta A 75 (2010) 428–436.
- [48] W.J. Geary, Coord. Chem. Rev. 7 (1971) 81–112.
- [49] M. Shebl, S.M.E. Khalil, F.S. Al-Gohani, J. Mol. Struct. 980 (2010) 78–87.
- [50] S.M.E. Khalil, M. Shebl, F.S. Al-Gohani, Acta Chim. Slov. 57 (2010) 716–725.
- [51] G.A.A. Al-Hazmi, M.S. El-Shahawi, I.M. Gabr, A.A. El-Asmy, J. Coord. Chem. 58 (2005) 713–733.
- [52] K.S. Abu-Melha, N.M. El-Metwally, Spectrochim. Acta A 70 (2008) 277–283.
- [53] N.M. El-Metwally, I.M. Gabr, A.M. Shallaby, A.A. El-Asmy, J. Coord. Chem. 58 (2005) 1145–1159.
- [54] M. Shebl, Spectrochim. Acta A 73 (2009) 313–323.
- [55] J.P. Jasinski, J.R. Bianchini, J. Cuva, F.A. El-Said, A.A. El-Asmy, D.X. West, Z. Anorg. Allg. Chem. 629 (2003) 202–206.
- [56] (a) B.J. Hathaway, D.E. Billing, Coord. Chem. Rev. 5 (1970) 143–207;
; (b) B.J. Hathaway, Struct. Bond. (Berlin) 57 (1984) 55–118.
- [57] C.J. Carrano, C.M. Nunn, R. Quan, J.A. Bonadies, V.L. Pecoraro, Inorg. Chem. 29 (1990) 944–951.
- [58] B. Jeragh, A.A. El-Asmy, Spectrochim. Acta A 129 (2014) 307–313.
- [59] M. Shebl, S.M.E. Khalil, S.A. Ahmed, H.A.A. Medien, J. Mol. Struct. 980 (2010) 39–50.
- [60] M. Shebl, S.M.E. Khalil, A. Taha, M.A.N. Mahdi, J. Mol. Struct. 1027 (2012) 140–149.
- [61] A.W. Coats, J.P. Redfern, Nature 201 (1964) 68–69.
- [62] A.H.M. Siddiggaiah, S.G. Naik, J. Mol. Struct. 582 (2002) 129–136.
- [63] C.R. Vinodkumar, M.K. Muraleedharan Nair, P.K. Radhakrishnan, J. Therm. Anal. Cal. 61 (2000) 143–149.
- [64] (a) M. Shebl, J. Mol. Struct. 1128 (2017) 79–93;
(b) B. Murukan, K. Mohanan, J. Enz. Inhib. Med. Chem. 22 (2007) 65–70.
- [65] K. Dhahagani, S.M. Kumar, G. Chakkavarthy, K. Anitha, J. Rajesh, A. Ramu, G. Rajagopal, Spectrochim. Acta A 117 (2014) 87–94.